lncRNA LUNAR1 accelerates colorectal cancer progression by targeting the miR-495-3p/MYCBP axis

JIAJIE QIAN[1], ALOK GARG[2], FUQIANG LI[3], QIANYUN SHEN[1] and KE XIAO[4]

[1]Department of Gastrointestinal Surgery, The First Affiliated Hospital, College of Medicine, Zhejiang University, Hangzhou, Zhejiang 310003, P.R. China; [2]Department of Surgery, City Hospital Braunschweig, D-38118 Braunschweig, Germany; [3]Department of Thyroid Surgery, The First Affiliated Hospital, College of Medicine, Zhejiang University, Hangzhou, Zhejiang 310003, P.R. China; [4]Institute of Molecular and Translational Therapeutic Strategies (IMTTS), Hannover Medical School, D-30625 Hannover, Lower Saxony, Germany

Received April 16, 2020; Accepted September 14, 2020

DOI: 10.3892/ijo.2020.5128

Abstract. Colorectal cancer (CRC) is a tumor type characterized by high patient morbidity and mortality. It has been reported that long non-coding (lncRNA) LUNAR1 (LUNAR1) participates in the regulation of tumor progression, such as diffuse large B-cell lymphoma. However, its role and underlying mechanisms in CRC progression have not been elucidated. The present study was designed to investigate the underlying mechanisms by which LUNAR1 regulates CRC progression. RT-qPCR and Pearson's correlation analysis revealed that LUNAR1 was highly expressed and was negatively associated with the overall survival of CRC patients. Moreover, CCK-8, clone formation, wound-healing migration, Transwell chamber and FACs assay analyses showed that LUNAR1 knockdown inhibited CRC cell proliferation, migration and invasion, while accelerating cell apoptosis. Additionally, LUNAR1 was found to function as a sponge of miR-495-3p, which was predicted by TargetScan and confirmed by luciferase reporter assay. Furthermore, functional studies indicated that miR-495-3p overexpression inhibited CRC cell proliferation, migration and invasion, while accelerating cell apoptosis. In addition, bioinformatics and luciferase reporter assays showed that miR-495-3p was found to negatively target Myc binding protein (MYCBP), and functional research showed that LUNAR1 accelerated CRC progression via the miR-495-3p/MYCBP axis. In conclusion, LUNAR1 accelerates CRC progression via the miR-495-3p/MYCBP axis, indicating that LUNAR1 may serve as a prognostic biomarker for CRC patients.

Correspondence to: Dr Ke Xiao, Institute of Molecular and Translational Therapeutic Strategies (IMTTS), Hannover Medical School, D-30625 Hannover, Lower Saxony, Germany
E-mail: xiao_ke_xiao@163.com

Abbreviations: CRC, colorectal cancer; lncRNA, long non-coding RNA; LUNAR1, lncRNA LUNAR1; ceRNA, competitive endogenous RNA; DMEM, Dulbecco's modified Eagle's medium; FBS, fetal bovine serum; miRNA, microRNA; Cox-2, cyclooxygenase 2; MMP-2, matrix metalloprotein 2; MMP-9, matrix metalloprotein 9; MYCBP, Myc binding protein

Key words: LncRNA LUNAR1, miR-495-3p, MYCBP, colorectal cancer

Introduction

Colorectal cancer (CRC) is a tumor type characterized by high patient morbidity and mortality (1). At present, surgery, radiotherapy and chemotherapy are the primary strategies for CRC treatment (2). Although some progress has been made in regards to CRC treatment on account of improvement in the medical level, the strong metastatic tendency of CRC still increases the risk of patient death (3). Notably, drug resistance and the generation of side effects are the primary obstacles for CRC treatment (4). Therefore, investigating the pathological progression of CRC is essential and beneficial to investigate new diagnostic and treatment strategies for CRC.

Long non-coding RNAs (lncRNAs), working as pivotal intracellular regulatory molecules, have functional bioactivity in various physiological processes (5). Crucially, lncRNAs have been proven to be pivotal regulators in tumor progression. In gastric cancer, lncRNA MAGI2-AS3 was found to be primarily distributed in the cytoplasm and was found to accelerate tumor progression by interacting with miR-141/200a (6). In cervical cancer, lncRNA SOX21-AS1 overexpression was found to inhibit cervical cancer progression, and its methylation was found to have clinical prognostic value (7). In prostate cancer, lncRNA SNHG7 was demonstrated to regulate tumor progression via the miR-324-3p/WNT2B axis (8). Consistently, reports indicate that multiple lncRNAs participate in the regulation of CRC processes. For example, lncRNA LEF1-AS1 was found to accelerate CRC progression by targeting the miR-489/DIAPH1 axis (9). lncRNA MIR503HG alleviated CRC progression by downregulating TGF-β2 expression (10). In addition, lncRNA TTN-AS1 accelerated CRC progression by sponging miR-376a-3p (11). LUNAR1 is a 491-nucleotide transcript located at 15q26.3, with 4 exons and a poly(A) tail (12). Increasing evidence indicates that LUNAR1 participates in tumor progression. In diffuse large

B-cell lymphoma, LUNAR1 was found to serve as a candidate prognostic biomarker via growth regulation (13). Moreover, the novel Notch-induced LUNAR1 promoted the proliferation of cancer cells, and may serve as a prognostic marker for CRC (14). These findings showed that LUNAR1 may act as an oncogene and plays an important role in cancer progression. However, to date, the roles of LUNAR1 in CRC progression have not been fully elucidated.

A microRNA (miRNA/mRNA) is defined as a series of non-coding RNA sequences of approximately 18-22 bp (15). Reports indicate that miRNAs play essential roles in gene expression via regulating post-transcriptional translation, which may be involved in the regulation of the progression of various diseases (16). Research has demonstrated that miR-495-3p participates in the regulation of the progression of multiple diseases. For example, miR-495-3p was found to inhibit rifampicin-induced SULT2A1 expression via accelerating the degradation of mRNAs, which in turn reduces hepatocellular toxicity (17). Increasing evidence indicates that miRNAs might be sponged by lncRNAs to regulate disease-related gene expression, resulting in the regulation of disease progression. Hence, lncRNAs may serve as competitive endogenous RNAs (ceRNAs) (18). For example, miR-495-3p is sponged by lncRNA NEAT1 to regulate STAT3 expression, resulting in alleviation of septicemia-related inflammatory response (19). Moreover, it is worth noting that miR-495-3p serves as an inhibitory regulator in CRC (20). However, the relationship between LUNAR1 and miR-495-3p, and the specific mechanisms involved remain unclear.

C-*myc* binding protein (MYCBP) plays a vital role in disease progression. MYCBP binds to the N-terminal region of MYC corresponding to the transactivation domain via its C-terminal region and stimulates the activation of E box-dependent transcription by c-MYC (21). In esophageal cancer, miR-26a and miR-26b inhibit tumor cell proliferation by inhibition of MYCBP expression (22). Overexpression of MYCBP binding protein was found to promote the invasion and migration of gastric cancer (23). These findings indicate that MYCBP plays a carcinogenic role in most cancers. In the present study, we further investigated the specific mechanism of MYCBP in CRC.

In this research, we aimed to explore the role of LUNAR1 in CRC progression and the underlying mechanisms by evaluating the proliferation, migration, invasion, and apoptosis of CRC cell lines, including SW480 and LoVo cells. Our findings suggest novel prognostic biomarkers for predicting the progression and prognosis of CRC.

Materials and methods

Patients. Fifteen CRC patients (age range, 25-60 years, average age, 42; 7 males and 8 females) at The First Affiliated Hospital, College of Medicine, Zhejiang University (Hangzhou, Zhejiang, China) between March 2018 and March 2019 were surveyed. These patients did not receive chemotherapy and radiotherapy before the operation; and did not present with diseases such as infectious diseases and multiple cancers. The clinical staging was based on the TNM analysis system of Union for International Cancer Control, UICC (version 8). All patients were informed before their inclusion; written consent of the patients was obtained. Multivariate analysis was performed to identify factors associated with overall survival using the Cox proportional hazards model.

Tissue specimens. Tumor tissues or corresponding paracancerous tissues were obtained by surgical extraction from 15 CRC patients (age range, 25-60 years, average age, 42; 7 males and 8 females) at The First Affiliated Hospital, College of Medicine, Zhejiang University (Hangzhou, Zhejiang, China) between March 2018 and March 2019. All experimental protocols were approved by the Ethics Committee of The First Affiliated Hospital, College of Medicine, Zhejiang University (Zhejiang, China; ethical approval no. PRO20180916-R1) and experimental procedures were conducted according to the Declaration of Helsinki Principles.

Cell culture. CRC cells lines, including HT29, LoVo, SW480, SW620 cells and normal HIEC cells which served as the control were obtained from Kunming Medical University (Kunming, Yunnan, China). Dulbecco's modified Eagle's medium (DMEM; Roche) supplemented with 10% fetal bovine serum (FBS) (Roche) and 1% penicillin-streptomycin solution (Solarbio) was applied to the cultured cells in a humid incubator containing 5% CO_2 at 37˚C.

Cell transfection. The transfection doses for pLKO.1 plasmid shRNAs targeting lncRNA LUNAR1, MYCBP and its negative control sh-NC (synthesized by Sangon Biotech) were 500 ng for cells in each well of 6-well plates. The transfection doses of miR-495-3p mimics or inhibitors (synthesized by Sangon Biotech), as well as their corresponding controls were 100 nM for cells in each well of 6-well plates. The transfection was performed using Lipofectamine™ 3,000 Transfection Reagent (Takara). Following a 48-h transfection, the SW480 and LoVo cells were applied to subsequent experiments. Detailed sequences for these shRNAs, mimics and inhibitors are presented in Table I.

RT-qPCR. Trizol reagent (Takara) was applied to extracted total RNA from CRC cell lines or tissues. M-MLV Reverse Transcriptase (RNase H) kit (Takara) was performed to synthesize cDNA. RT-qPCR was performed as previously described (24). Primers applied to this research are shown in Table II.

Subcellular fractionation analysis. PARIS™ kit (Invitrogen; Thermo Fisher Scientific, Inc.) was applied for subcellular fractionation analysis, according to the manufacturer's instructions. Nuclear and cytoplasmic extraction reagents (Beyotime Institute of Biotechnology) were applied to separate cytoplasm and nuclear grade from SW480 or LoVo cells. RT-qPCR was conducted to analyze cytoplasmic and nuclear RNA extracts; GAPDH and U6 served as normalizing controls, respectively.

Western blot analysis. Total proteins were isolated from SW480 and LoVo cells which were transfected with corresponding plasmids by using cell lysis buffer (Beyotime Institute of Biotechnology). Western blot analysis was conducted as previously described (25). All antibodies, including cyclin D1 (ab16663), p21 (ab109520), Bax (ab32503), Bcl-2 (ab32124), cleaved-caspase 3 (ab2302), cleaved-caspase 9 (ab2324), Cox-2

Table I. Detailed information regarding the sequences of the miRNA mimics, inhibitors and shRNAs.

Sequence name	Sequences (5'-3')
miR-495-3p mimics	5'-AAACAAACATGGTGCACTTCTT-3'
NC mimics	5'-ATCGTGCTAGTCGATGCTAGCT-3'
miR-495-3p inhibitors	5'-GCTTTATATGTGACGAAACAA-3'
NC inhibitors	5'-CGATCGCAGCGGTGCAGTGCG-3'
sh-LncRNA LUNAR1	5'-GCCTGTTGAGTCACAGTTTCC-3'
sh-MYCBP	5'-GCCCATTACAAAGCCGCCGAC-3'
sh-NC	5'-CGATGTCGTAGCTGACTGACG-3'

NC, negative control; lncRNA, long non-coding RNA; MYCBP, Myc binding protein.

Table II. Primer sequences.

Primer name	Primer sequences (5'-3')
F-LUNAR1	5'-CTCAGTAGCTCTCTCTCTCTCTCTCT CT-3'
R-LUNAR1	5'-TTGTCTCCCTAGATATCA-3'
F-MYCBP	5'-ATGGCCCATTA CAAGCCGC-3'
R-MYCBP	5'-CTATTCAGCG CTCTCTCTCTCTCT-3'
F-GAPDH	5'-GAGTCAACGGATTTGGTCGT-3'
R-GAPDH	5'-TTGATTTTGGAGGGATCTCG-3'
F-miR-495-3p	5'-AAACAAACAUGGUGCACUUCUU-3'
R-miR-495-3p	5'-GAAGUGCACCAUGUUUGUUUUU-3'
F-U6	5'-CTCGCTTCGGCAGCACA-3'
R-U6	5'-AACGCTTCACGAATTTGCGT-3'

F, forward; R, reverse; MYCBP, Myc binding protein; GAPDH, glyceraldehyde 3-phosphate dehydrogenase.

(ab179800), MMP-2 (ab92536), MMP-9 (ab76003), MYCBP (ab86078) and GAPDH (ab9485) used in this research were obtained from Abcam (dilution, 1:1,000). The optical density of protein bands was quantified by Image J software1.8.0 (National Institutes of Health, Bethesda, MD, USA).

CCK-8 assay. SW480 or LoVo cell proliferation was analyzed by Cell Counting Kit-8 (Roche) according to the manufacturer's instructions.

Colony formation assay. Long-term cell proliferation was detected by colony formation assay. In detail, SW480 and LoVo cells were added into 12-well plates, at a dose of 50 cells per well. Dishes were taken out when the cell colonies in each well were more than 25. The numbers of cell clones were counted following staining with 1% crystal violet for 5 min at room temperature, and images were captured by an optical microscope (Olympus, CX23).

FACs analysis. A total of $1x10^5$ SW480 or LoVo cells were cultured in 12-well plate by using serum-free DMEM for 24 h, centrifuged at 150 x g for 5 min, and washed twice with pre-cooled 1X PBS. Subsequently, the cells were fixed with 70% ethanol (Solarbio), maintained at 20˚C for 15 min, centrifuged at 150 x g for 5 min, and washed twice with pre-chilled 1X PBS. Next, the cells were incubated with 10 μg/μl DNase-free RNaseA (Sigma-Aldrich; Merck KGaA) for 45 min at 37˚C to eliminate RNA, and washed twice with pre-chilled 1X PBS. Finally, following centrifuging at 150 x g for 5 min, the cells were incubated with 1 mg/ml iodide (Sigma-Aldrich; Merck KGaA) in the dark at 4˚C for 12 min. The cell distribution at each phase of the cell cycle was quantified in a flow cytometer and using ModFit software 3.3 (Verity Software House). In addition, according to the manufacturer's instructions, Annexin-FITC/PI Apoptosis Detection Kit (Beyotime Institute of Biotechnology) was combined with flow cytometry to detect cell apoptosis (19). ModFit software 3.3 was performed to analyze the data.

Wound-healing migration assay. SW480 and LoVo cells, which were transfected with corresponding plasmids, were applied to the wound-healing assay. The detailed procedure was described previously (26).

Transwell chamber assay. A Transwell chamber with a membrane with pores of 8 μm in diameter was applied to assess cell migration. Specific operation protocol has been previously described (27).

RIP (RNA immunoprecipitation) assay. In detail, RNA immunoprecipitation was performed using the EZ-Magna RIP kit (Millipore) following the manufacturer's protocol. SW480 and LoVo cells at 80-90% confluency was scraped off, and then were lysed in complete RIP lysis buffer, after which 100 μl of whole cell extract was incubated with RIP buffer containing magnetic beads conjugated with human anti-Ago2 antibody (Sigma-Aldrich; Merck KGaA, 04-642) and negative control normal mouse IgG (Sigma-Aldrich; Merck KGaA, 12-371). Anti-SNRNP70 (Sigma-Aldrich; Merck KGaA, SAB1305762) was used as a positive control for the RIP procedure. Samples were incubated with Proteinase K with shaking to digest the protein and then immunoprecipitated RNA was isolated. The RNA concentration was measured using a NanoDrop (Thermo Fisher Scientific, Inc.) and the RNA quality was assessed using a bioanalyzer (Agilent Technologies, Inc.). Furthermore, purified RNA was subjected to RT-qPCR analysis to demonstrate the presence of the binding targets using respective primers.

Bioinformatics and luciferase reporter assay. TargetScan (www.targetscan.org) was conducted to predict the underlying target genes. The dual-luciferase reporter assay was performed as previously described (28).

Statistical analysis. The data are expressed as mean ± SD as represented from three independent experiments, and GraphPad Prism version 5.0 software (GraphPad Software, Inc.) was used for statistical analysis of all data. Pearson's correlation was performed to evaluate potential correlations between groups (Pearson's rho). Student's t test or one-way

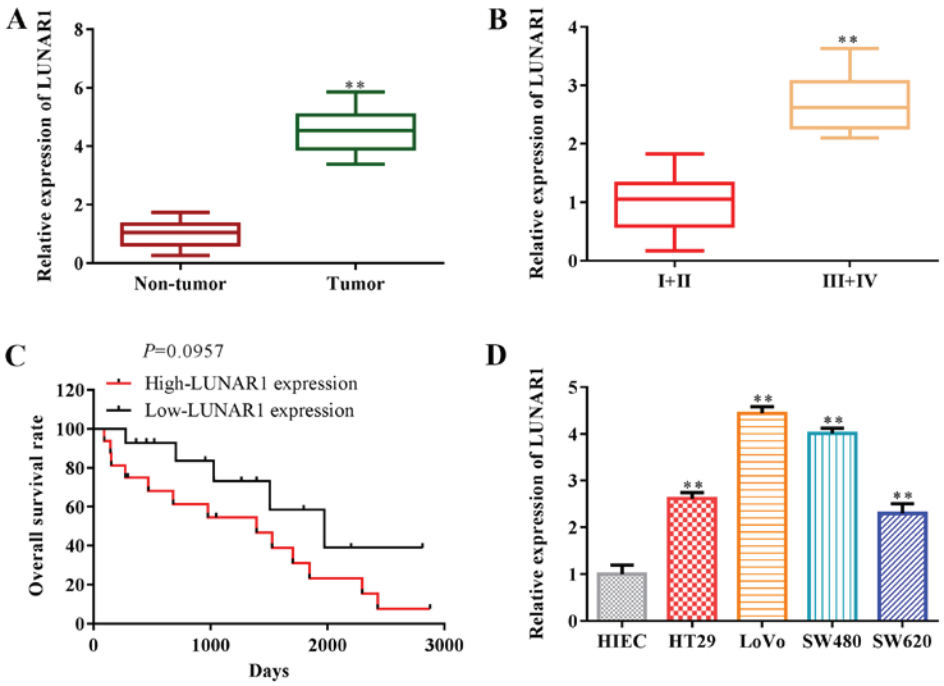

Figure 1. LUNAR1 is highly expressed and is associated with the poor prognosis of CRC patients. (A and B) RT-qPCR was performed to assess the RNA level of LUNAR1 in CRC tissues vs. non-tumor tissues. **P<0.01 vs. non-tumor tissues. (B) RT-qPCR was performed to assess the RNA level of LUNAR1 in CRC tissues with stage I+II (n=7) and III+IV (n=8). **P<0.01 vs. I+II stage tumors. (C) Association of LUNAR1 expression with patient overall survival times (n=15). (D) LUNAR1 expression in CRC cell lines, including HT29, LoVo, SW480, SW620 cells; HIEC cells served as a negative control. **P<0.01 vs. HIEC control cells. All comparisons were performed using paired t-test or one-way ANOVA. Error bars represent SD. Data represent three independent experiments. LUNAR1, lncRNA LUNAR1.

ANOVA was used for comparison between two groups, and Tukey post-test was used for comparison between multiple groups. P-value <0.05 was indicative of a statistically significant difference.

Results

LUNAR1 is highly expressed and associated with overall survival of the CRC patients. It has been reported that LUNAR1 participates in the progression of various tumor types, such as diffuse large B-cell lymphoma (13). To explore the roles of LUNAR1 in CRC, RT-qPCR was performed to assess LUNAR1 expression in CRC tissues and cell lines. The findings revealed that LUNAR1 expression was significantly upregulated in the tumor tissues, compared with that in non-tumor tissues (P<0.01; Fig. 1A), and LUNAR1 expression in low-grade tumor tissues (n=7; 4 male, 3 female) was lower than that in high-grade tumor tissues (n=8; 4 male, 4 female) (P<0.01; Fig. 1B). Overall survival rate analysis indicated that LUNAR1 expression was negatively associated with overall survival in the CRC patients (P=0.0957; Fig. 1C). LUNAR1 was upregulated in CRC cell lines, including HT29, LoVo, SW480, SW620, compared with the control HIEC cells (P<0.01; Fig. 1D). Note that we selected two types of CRC cells, including SW480 and LoVo cells in subsequent research, since LUNAR1 was significantly upregulated in these cells. Collectively, LUNAR1 was found to be highly expressed and associated with the overall survival of the CRC patients, indicating that LUNAR1 serves as a prognostic biomarker for CRC patients.

LUNAR1 knockdown inhibits CRC cell proliferation and accelerates cell apoptosis. To further explore the roles of LUNAR1 in CRC cell proliferation, sh-LUNAR1 was transfected into SW480 and LoVo cells for LUNAR1 knockdown. RT-qPCR analysis indicated that LUNAR1 was significantly knocked down following sh-LUNAR1 transfection (P<0.01; Fig. 2A). CCK-8 assay analysis indicated that LUNAR1 knockdown significantly inhibited cell viability in the SW480 and LoVo cells, compared to the control cells (P<0.01; Fig. 2B). Consistently, colony formation assay revealed that LUNAR1 knockdown inhibited cell proliferation, compared to the control in both cell lines (P<0.01; Fig. 2C). Cell cycle analysis was performed to verify whether the decrease in cell viability was caused by cell cycle arrest or apoptosis. FACS analysis showed that LUNAR1 knockdown arrested the cell cycle in the G1 phase (P<0.05; Fig. 2D), which was further verified by western blot analysis. In brief, LUNAR1 knockdown significantly inhibited the levels of cyclin D1 and cyclin E proteins, while increasing p21 and p27 protein expression (P<0.01; Fig. 2E). Furthermore, FACs analysis indicated that LUNAR1 knockdown accelerated cell apoptosis, compared to the control (P<0.01; Fig. 2F). Consistently, LUNAR1 knockdown upregulated the levels of Bax, cleaved-caspase 3 and cleaved-caspase 9 proteins, and inhibited Bcl-2 protein expression (P<0.01; Fig. 2G). Taken together, LUNAR1 knockdown inhibited CRC cell proliferation and accelerated apoptosis.

LUNAR1 knockdown inhibits CRC cell migration and invasion. Excessive migration and invasion of tumor cells is a hallmark of cancer (29). Therefore, to investigate the roles of LUNAR1 in CRC cell migration and invasion, sh-LUNAR1 was transfected into SW480 and LoVo cells in order to knock down LUNAR1. Wound-healing migration assay showed that LUNAR1 knockdown inhibited cell migration of the SW480

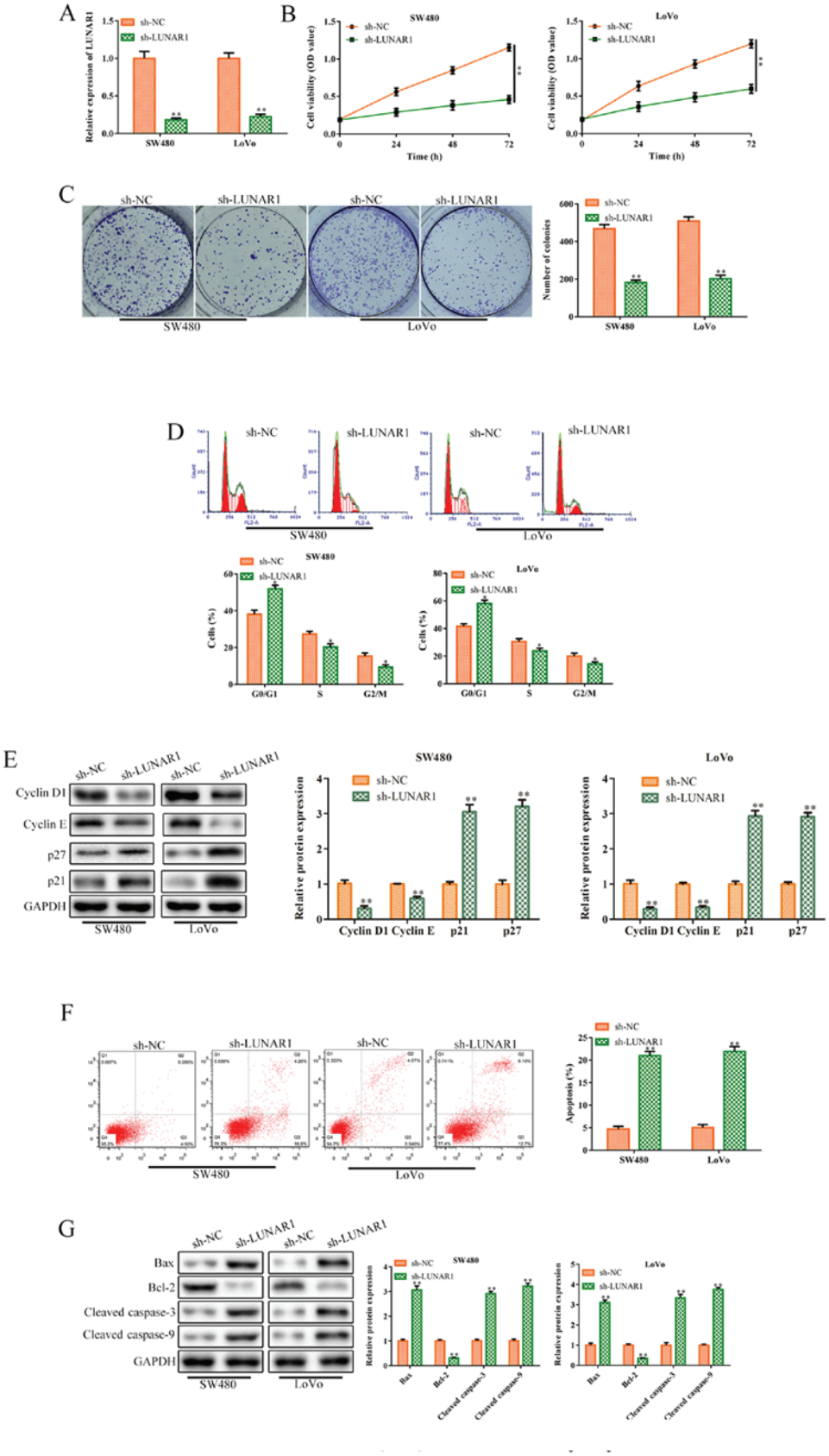

Figure 2. LUNAR1 knockdown inhibits CRC cell proliferation and accelerates apoptosis. SW480 and LoVo cells were transfected with sh-LUNAR1 for 24 h to promote LUNAR1 knockdown, and sh-NC served as a negative control. (A) RT-qPCR was performed to detect LUNAR1 expression following transfection. (B) CCK-8 assay was performed to evaluate SW480 and LoVo cell viability. (C) Colony formation assay was conducted to assess SW480 and LoVo cell proliferation. (D) FACS analysis was performed to analyze cell cycle distribution. (E) Western blot analysis was performed to detect the levels of cell cycle-related proteins, including cyclin D1, cyclin E, p27 and p21. (F) Apoptosis analysis was performed to evaluate cell apoptosis. (G) Western blot analysis was conducted to measure the levels of apoptosis-related proteins, including Bax, Bcl2, cleaved-caspase 3 and cleaved-caspase 9. **P<0.01 vs. the sh-NC group. Comparisons were performed using paired t-test or one-way ANOVA. Error bars represent SD. Data represent three independent experiments. LUNAR1, lncRNA LUNAR1; CRC, colorectal cancer.

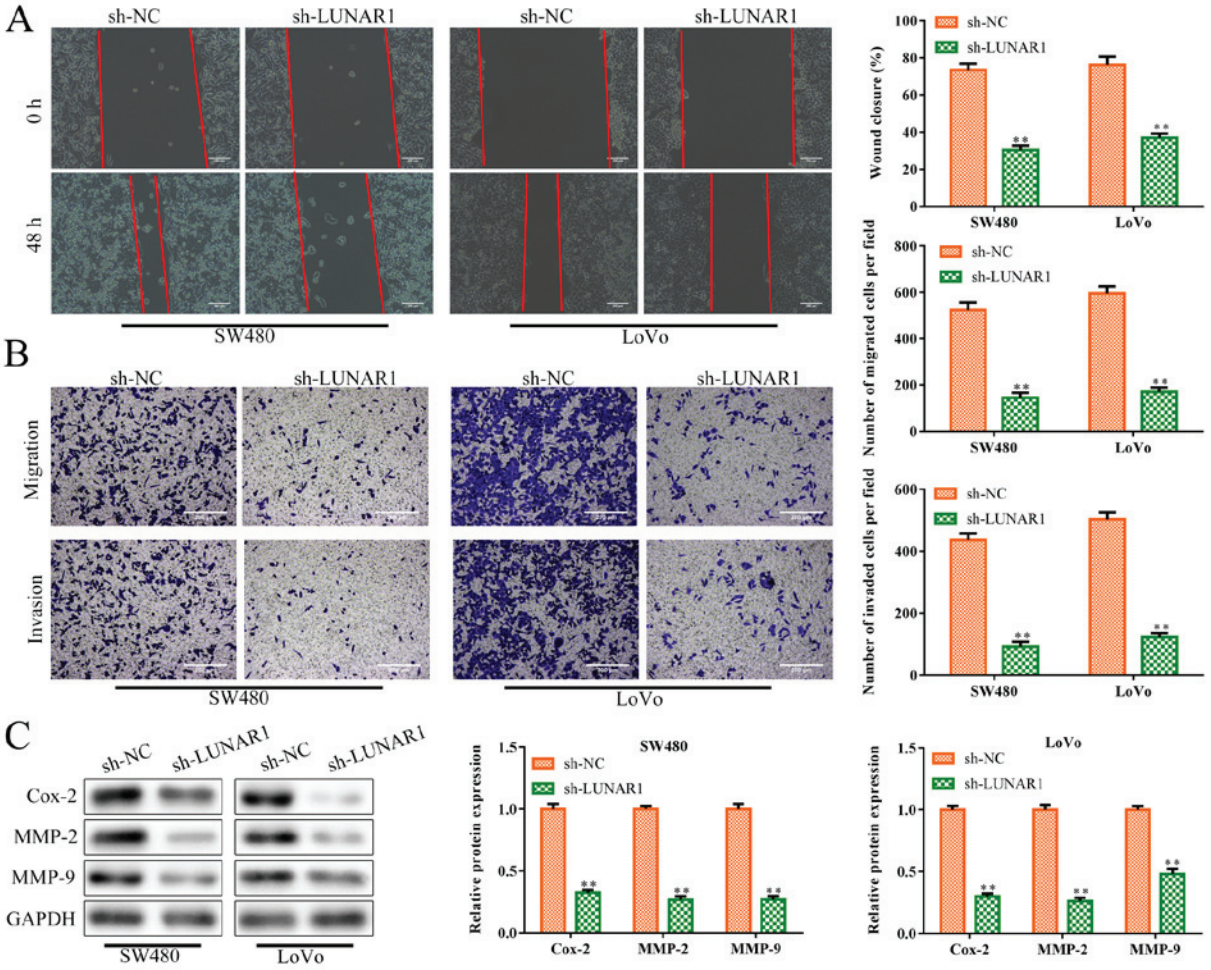

Figure 3. LUNAR1 knockdown inhibits CRC cell migration and invasion. SW480 and LoVo cells were transfected with sh-LUNAR1 for 24 h to promote LUNAR1 knockdown, and sh-NC served as a negative control. (A) Wound-healing migration assay was conducted to assess cell migration. (B) Transwell chamber assay was performed to evaluate cell migration and invasion. (C) Western blot analysis was performed to detect the levels of invasion-related proteins, including Cox-2, MMP-2 and MMP-9. **P<0.01 vs. the sh-NC group. Comparisons were performed using paired t-test or one-way ANOVA. Error bars represent SD. Data represent three independent experiments. LUNAR1, lncRNA LUNAR1; CRC, colorectal cancer; Cox-2, cyclooxygenase 2; MMP-2, matrix metalloprotein 2; MMP-9, matrix metalloprotein 9.

and LoVo cells, compared to the controls (P<0.01; Fig. 3A). Similarly, as shown in Fig. 3B, LUNAR1 knockdown inhibited cell migration and invasion abilities (P<0.01). Simultaneously, western blot analysis (Fig. 3C) showed that the levels of invasion-related proteins were inhibited in the SW480 and LoVo cells by LUNAR1 knockdown (P<0.01), including cyclooxygenase 2 (Cox-2), matrix metalloprotein (MMP)-2 and MMP-9, which play pivotal roles in angiogenesis and tumor metastasis (30). Collectively, LUNAR1 knockdown inhibited CRC cell migration and invasion, indicating that LUNAR1 plays an active role in CRC progression.

LUNAR1 functions as a sponge of miR-495-3p in CRC cells. As is known, lncRNAs may function as a ceRNA of miRNA, and their subcellular localization is closely related to the biological effects (31). Therefore, subcellular fractionation analysis was performed to detect LUNAR1 subcellular distribution in the SW480 and LoVo cells. RT-qPCR analysis indicated that LUNAR1 was highly expressed in the cytoplasm and slightly expressed in the nucleus (P<0.01; Fig. 4A), indicating that LUNAR1 primarily exerted its biological functions in the cytoplasm of SW480 and LoVo cells. In addition, research has shown that miR-495-3p serves as an inhibitory regulator in the progression of various tumors (19). In the present paper, bioinformatics analysis indicated a putative interaction between LUNAR1 and miR-495-3p, and the luciferase reporter assay confirmed that miR-495-3p mimics decreased the luciferase activity of the wild-type (WT) 3'UTR of LUNAR1 in both SW480 and LoVo cell lines, whereas this inhibition was blocked when the putative binding sites were mutated (Mut) (P<0.01; Fig. 4B and C). Furthermore, RT-qPCR analysis indicated that miR-495-3p was downregulated in the CRC tissues and cell lines, including HT29, LoVo, SW480, SW620 cells, when compared to the non-tumor tissues and control NIEC cells (P<0.05; Fig. 4D and E). As shown in Fig. 4F, the interaction between LUNAR1 and miR-495-3p was further verified by RIP assay where both LUNAR1 and miR-495-3p were enriched in AGO2 immunoprecipitants compared with that of IgG group (P<0.001). In addition, RT-qPCR analysis showed that LUNAR1 knockdown significantly accelerated miR-495-3p expression in SW480 and LoVo cells (P<0.01), and Pearson's correlation analysis showed that the level of LUNAR1 was negatively correlated with miR-495-3p in SW480 and LoVo cells (R=0.44; P=0.014; Fig. 4G and H).

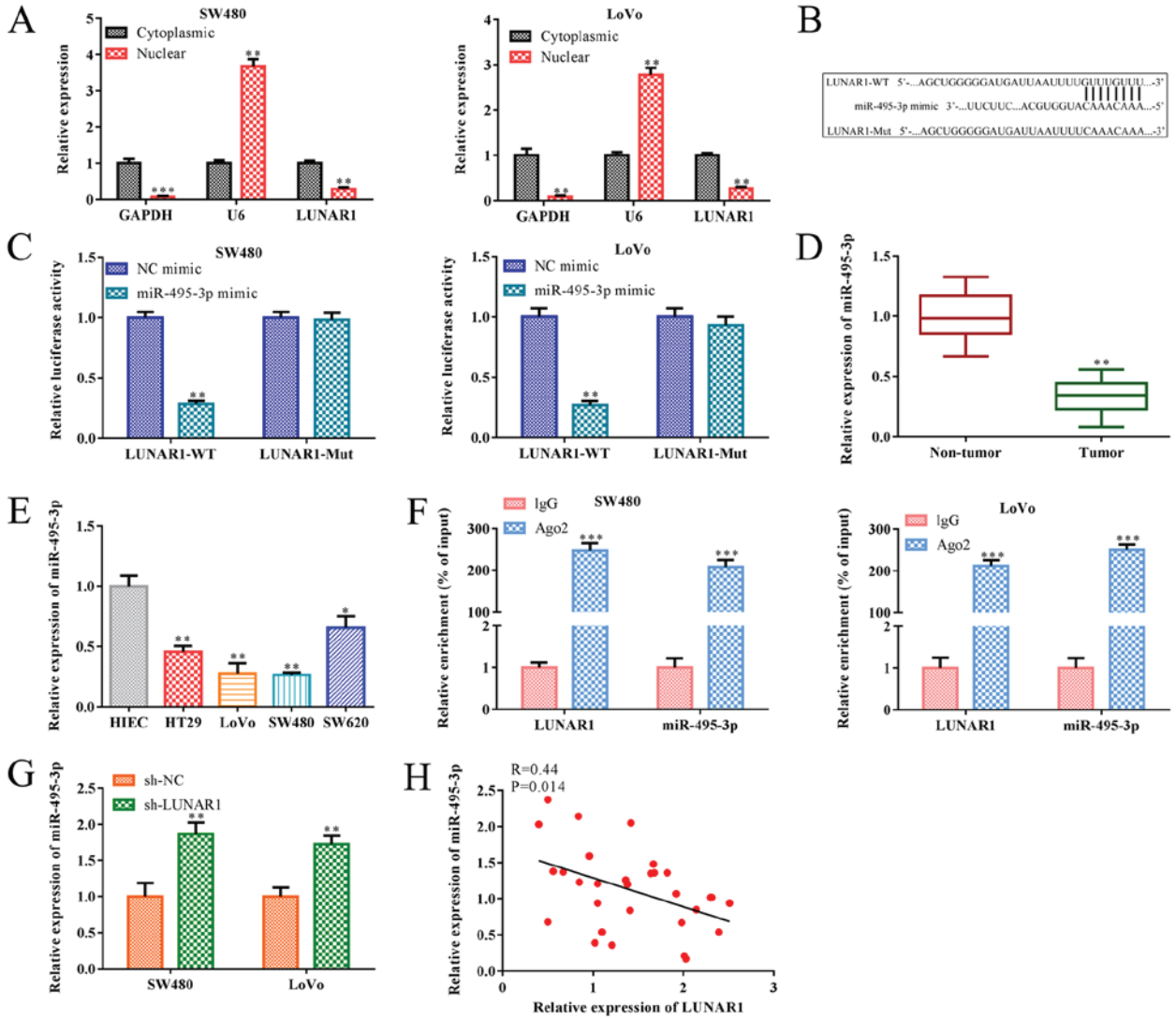

Figure 4. LUNAR1 functions as a sponge of miR-495-3p. Cytoplasm and nuclear grades were separated from SW480 and LoVo cells. (A) RT-qPCR was performed to assess the levels of U6 and LUNAR1 in the cytoplasm and nuclei. **P<0.01, ***P<0.001 vs. cytoplasmic LUNAR1. (B) Potential binding site between miR-495-3p and LUNAR1 was predicted by TargetScan software. miR-495-3p mimics were transfected into SW480 and LoVo cells for 24 h; NC mimics served as a control. (C) Dual luciferase reporter gene assay was performed to confirm the direct binding relationship between miR-495-3p and LUNAR1. **P<0.01 vs. the NC mimic group. (D) RT-qPCR was carried to detect the RNA level of miR-495-3p in CRC and non-tumor tissues. **P<0.01 vs. the non-tumor tissues. (E) RT-qPCR was carried to detect the RNA level of miR-495-3p in CRC cell lines; HIEC cells served as the control. *P<0.05, **P<0.01 vs. the HIEC cells. (F) Interaction between LUNAR1 and miR-495-3p was determined by RIP assay. ***P<0.001 vs. the IgG group. SW480 and LoVo cells were transfected with sh-LUNAR1 for LUNAR1 knockdown for 24 h, and sh-NC served as a negative control. (G) RT-qPCR was performed to assess miR-495-3p RNA levels. **P<0.01 vs. the sh-NC group. (H) Pearson's correlation analysis was conducted to analyze the correlation between LUNAR1 and miR-495-3p in SW480 and LoVo cells. Comparisons were performed using paired t-test or one-way ANOVA. Error bars represent SD. Data represent three independent experiments. LUNAR1, lncRNA LUNAR1; CRC, colorectal cancer.

Taken together, LUNAR1 affects the dysregulation of miR-495-3p via the sponging in CRC cells.

miR-495-3p overexpression inhibits CRC cell proliferation, migration and invasion, and promotes apoptosis. It has been reported that miR-495-3p participates in the regulation of tumor cell bioactivity. For example, miR-495-3p regulates osteosarcoma cell apoptosis by targeting C1q/TNF-related protein 3 (32). To investigate the roles of miR-495-3p in CRC cell proliferation, miR-495-3p was effectively overexpressed in the SW480 and LoVo cells (P<0.01; Fig. 5A). CCK-8 and colony formation assays indicated that SW480 and LoVo cell proliferation was inhibited by miR-495-3p overexpression, compared to the control (NC mimic group) (P<0.01; Fig. 5B and C). In accordance with these results, miR-495-3p overexpression accelerated SW480 and LoVo cell apoptosis, compared with the control (P<0.01; Fig. 5D). Furthermore, Transwell chamber assays indicated that SW480 and LoVo cell migration and invasion were significantly inhibited by miR-495-3p overexpression, compared with the NC mimic groups (P<0.01; Fig. 5E). Collectively, miR-495-3p overexpression inhibited CRC cell proliferation, migration and invasion, and promoted apoptosis, further indicating that miR-495-3p suppresses CRC progression.

miR-495-3p negatively targets MYCBP. miRNAs participate in the regulation of tumor progression by regulating the

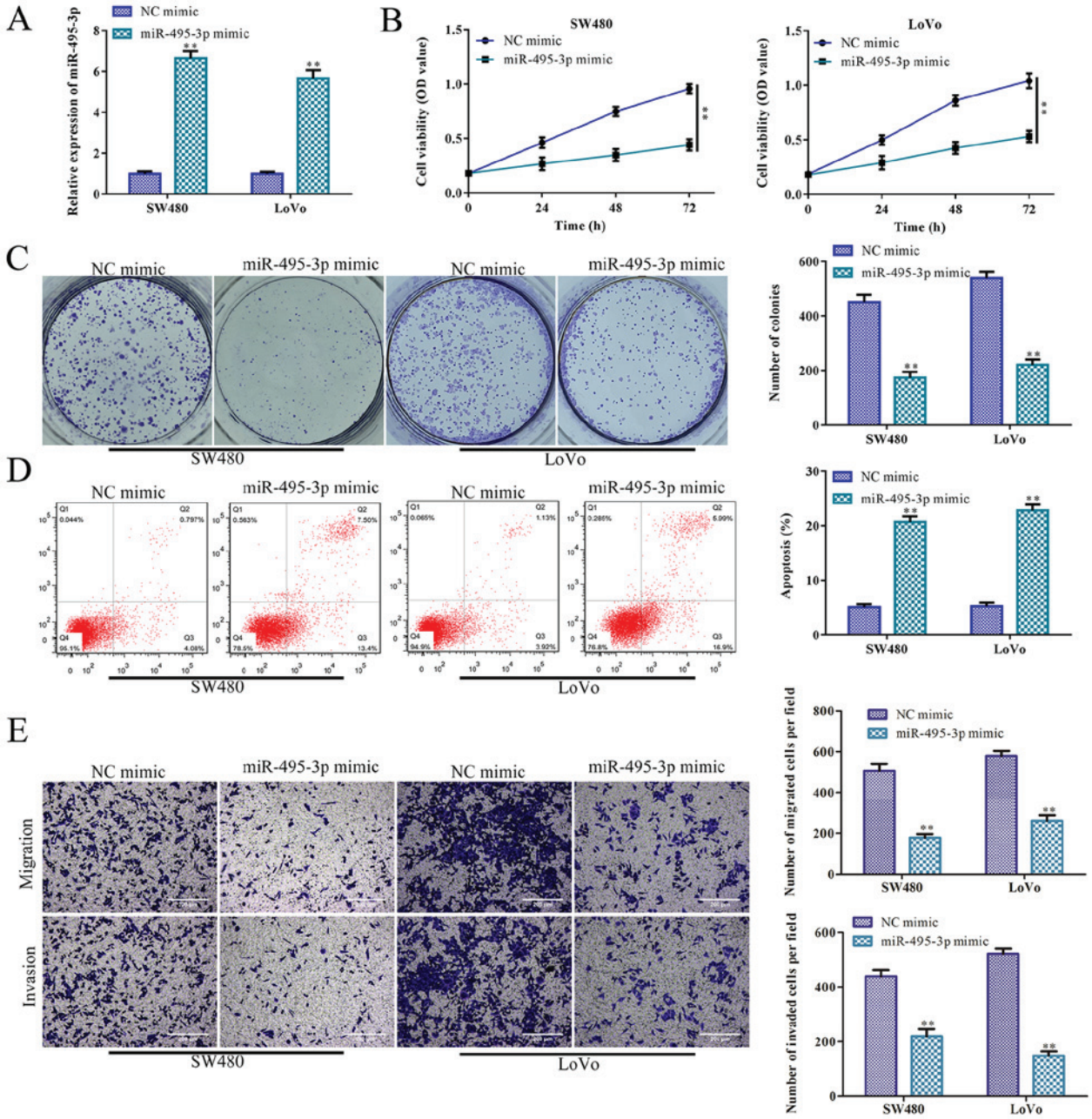

Figure 5. miR-495-3p overexpression inhibits CRC cell proliferation and invasion, and promotes apoptosis. SW480 and LoVo cells were transfected with miR-495-3p mimics for 24 h to promote miR-495-3p overexpression; NC mimic served as a negative control. (A) RT-qPCR was carried to assess miR-495-3p RNA levels. (B) CCK-8 assay was performed to evaluate cell viability. (C) Colony formation assay was conducted to assess cell proliferation. (D) Apoptosis analysis was conducted to assess cell apoptosis. (E) Transwell chamber assays were carried to assess cell migration and invasion. **P<0.01 vs. the NC mimic group Comparisons were performed using paired t-test or one-way ANOVA. Error bars represent SD. Data represent three independent experiments. CRC, colorectal cancer.

post-transcriptional translation of target genes (33). To verify the downstream regulator of miR-495-3p in CRC, bioinformatics analysis was applied to predict the putative target gene of miR-495-3p. The findings indicated that a binding site of miR-495-3p was observed in 3' UTR (untranslated region) of MYCBP (Fig. 6A), which resides on chromosome 1p and its tumor-promoting effect was confirmed. Subsequently, the luciferase reporter assay confirmed this prediction. Reduced luciferase activity was observed in the SW480 and LoVo cells co-transfected with wild-type (WT) plasmids of MYCBP and miR-495-3p mimics, whereas this trend was blocked when the putative binding sites were mutated (Mut) (P<0.01; Fig. 6B). RT-qPCR analysis indicated that MYCBP expression was upregulated in the CRC tissues and cell lines, including HT29, LoVo, SW480, SW620 cells when compared with the non-tumor tissue and HIEC cell line (P<0.01; Fig. 6C and D). Meanwhile, miR-495-3p overexpression inhibited the MYCBP levels in the SW480 and LoVo cells, compared to the NC mimic group (P<0.01; Fig. 6E). Consistently, western blot analysis indicated that miR-495-3p overexpression inhibited MYCBP expression in the SW480 and LoVo cells, compared to the control (P<0.01; Fig. 6F). Furthermore, Pearson's correlation analysis showed that MYCBP was negatively associated with miR-495-3p in the

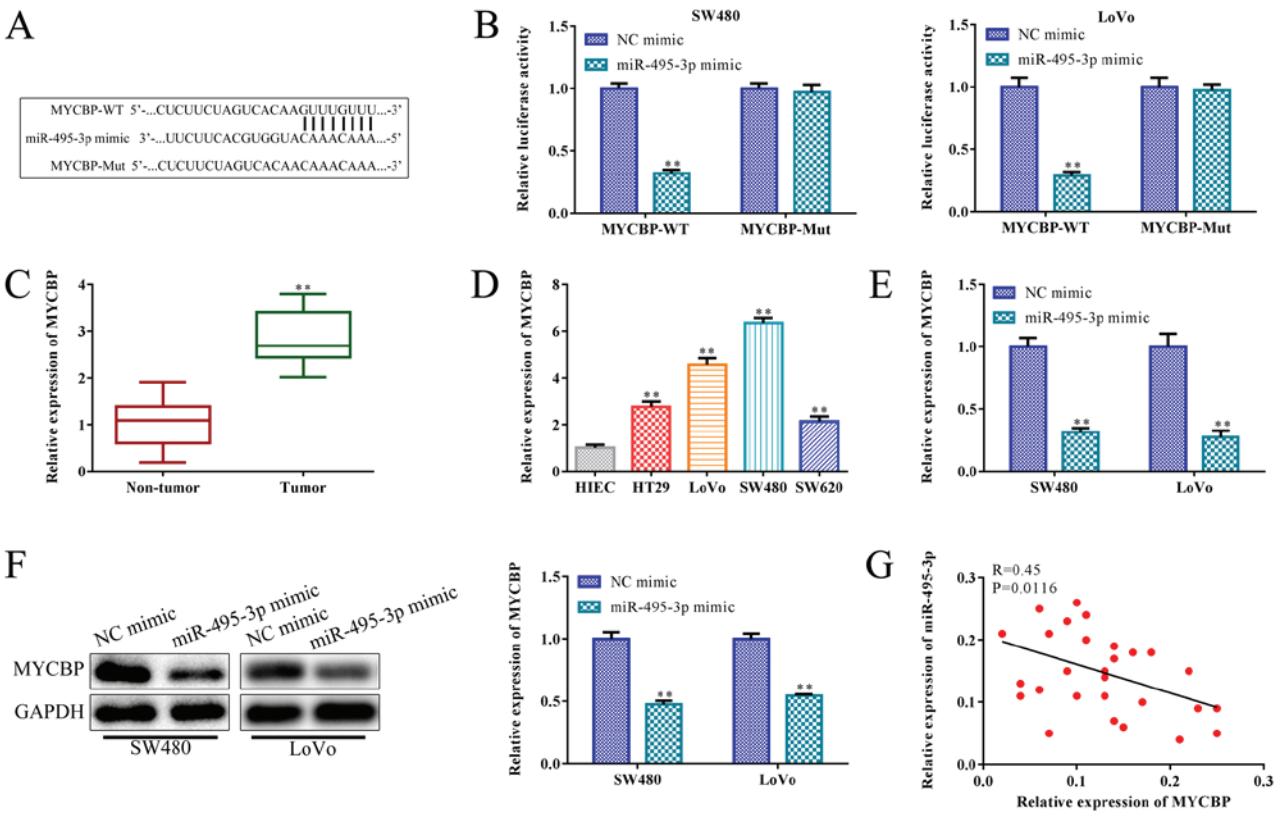

Figure 6. miR-495-3p negatively targets MYCBP. (A) Potential binding site between miR-495-3p and MYCBP was predicted by TargetScan software. miR-495-3p mimics were transfected into SW480 and LoVo cells; NC mimic served as a control. (B) Dual luciferase reporter gene assay was performed to confirm the direct binding relationship between miR-495-3p and MYCBP. **P<0.01 vs. the NC mimic group. (C) RT-qPCR was carried to detect MYCBP expression in CRC and non-tumor tissues. **P<0.01 vs. the non-tumor tissues. (D) RT-qPCR was carried to detect MYCBP expression in CRC cell lines and normal control HIEC cells. **P<0.01 vs. the HIEC cells. (E) RT-qPCR was performed to assess MYCBP mRNA levels in SW480 and LoVo cells, following miR-495-3p overexpression. **P<0.01 vs. the NC mimic group. (F) Western blot analysis was conducted to measure the levels of MYCBP protein in SW480 and LoVo cells, following miR-495-3p overexpression. **P<0.01 vs. the NC mimic group. (G) Pearson's correlation analysis was performed to analyze the correlation between miR-495-3p and MYCBP in SW480 and LoVo cells. Comparisons were performed using paired t-test or one-way ANOVA. Error bars represent SD. Data represent three independent experiments. MYCBP, Myc binding protein; CRC, colorectal cancer.

SW480 and LoVo cells (R=0.45; P=0.0116; Fig. 6G). Taken together, miR-495-3p negatively targets MYCBP in SW480 and LoVo cells.

LUNAR1 accelerates CRC progression via the miR-495-3p/MYCBP axis. Based on the above results, rescue assays were performed to demonstrate whether LUNAR1 exerts its function in CRC via the miR-495-3p/MYCBP axis. RT-qPCR analysis indicated that the increased expression of miR-495-3p promoted by sh-LUNAR1 was reversed by the miR-495-3p inhibitor in the SW480 and LoVo cells. In addition, the increased expression of miR-495-3p promoted by sh-LUNAR1 was also reversed by sh-MYCBP in the SW480 and LoVo cells (P<0.01; Fig. 7A).

CCK-8 and colony formation assays depicted that LUNAR1 knockdown-induced reduction in cell proliferation ability of SW480 and LoVo cells was promoted by miR-495-3p inhibitors, whereas such an impact of miR-459-3p inhibitors was subsequently recovered by MYCBP depletion (P<0.05; Fig. 7B and C). Furthermore, FACs analysis indicated that LUNAR1 knockdown-induced cell apoptosis was abolished by miR-495-3p inhibitors, while MYCBP knockdown antagonized the effect of miR-495-3p inhibitors in the LUNAR1-knockdown SW480 and LoVo cells (P<0.05; Fig. 7D). Similar results were observed in the migration and invasion abilities of the SW480 and LoVo cells (P<0.05; Fig. 7E). Collectively, LUNAR1 accelerates CRC progression via targeting the miR-495-3p/MYCBP axis.

Discussion

Currently, various diagnostic and therapeutic strategies have been applied to the treatment of CRC. However, the overall survival rate of CRC patients remains unsatisfactory (34). Thus, the search for novel molecular biomarkers for CRC may contribute to the improvement of clinical treatment (2). In the present study, we elucidated the specific mechanisms through which LUNAR1 accelerates CRC progression. Our findings demonstrated that LUNAR1 accelerated CRC progression via the miR-495-3p/MYCBP axis, indicating that LUNAR1 may serve as a prognostic biomarker for CRC patients.

Long non-coding (lnc.) RNAs are defined as a novel class of non-protein coding RNA with a length of over 200 nt, which are involved in the regulation of multiple molecular functions (35). Increasing evidence reveals that lncRNAs regulate the post-transcriptional translation of genes by sponging miRNAs, thus playing a vital role in the pathological process

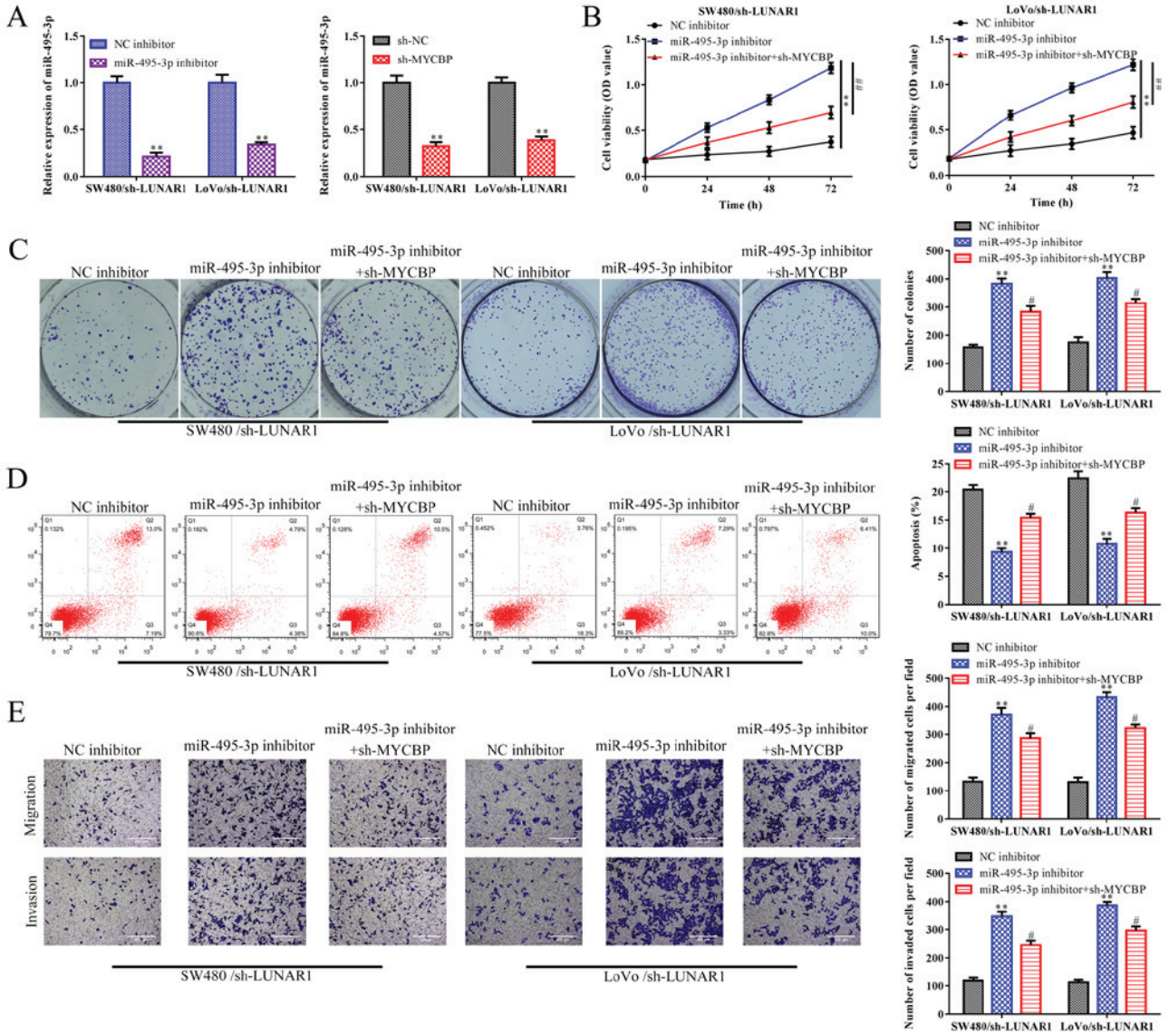

Figure 7. LUNAR1 accelerates CRC progression via the miR-495-3p/MYCBP axis. miR-495-3p inhibitors or sh-MYCBP plasmids were transfected into SW480 and LoVo cells transfected with sh-LUNAR1 for 48 h; NC inhibitors or sh-NC served as the control. (A) RT-qPCR was performed to detect miR-495-3p. **P<0.01 vs. the NC inhibitor or sh-NC group. (B) CCK-8 was carried to assess cell viability. **P<0.01, miR-495-3p inhibitor vs. NC inhibitor; $^{\#\#}$P<0.01, miR-495-3p inhibitor+sh-MYCBP vs. miR-495-3p inhibitor. (C) Colony formation assay was performed to evaluate cell proliferation. **P<0.01 vs. NC inhibitor group, $^{\#}$P<0.05 vs. miR-495-3p inhibitor group. (D) Apoptosis analysis was carried out to detect cell apoptosis. **P<0.01 vs. NC inhibitor group, $^{\#}$P<0.05 vs. miR-495-3p inhibitor group. (E) Transwell chamber assays were conducted to evaluate cell migration and invasion. **P<0.01 vs. NC inhibitor group, $^{\#}$P<0.05 vs. miR-495-3p inhibitor group. Comparisons were performed using paired t-test or one-way ANOVA. Error bars represent SD. Data represent three independent experiments. LUNAR1, lncRNA LUNAR1; CRC, colorectal cancer; MYCBP, Myc binding protein.

of various diseases (13). LUNAR1 is a transcription of 491 nucleotides at 15q26.3 with 4 exons and a poly(A) tail (14). Research has found that LUNAR1 regulates disease progression via sponging miRNAs, such as acute leukemia and diffuse large B-cell lymphoma (13). In the present study, our findings indicated that LUNAR1 is highly expressed and negatively associated with the overall survival of CRC patients, indicating that LUNAR1 serves as a prognostic biomarker for CRC patients. In addition, LUNAR1 knockdown inhibited CRC cell proliferation, migration and invasion, and accelerated cell apoptosis. Our findings indicated that LUNAR1 plays an active role in CRC progression. Mechanistically, LUNAR1 functioned as a sponge of miR-495-3p, and miR-495-3p overexpression inhibited CRC cell progression. Hence, LUNAR1 accelerated CRC progression by sponging miR-945-3p.

Myc binding protein (MYCBP), belonging to the Myc family is located on chromosome 1p (36). It has been reported that MYCBP, as a co-activator of c-Myc, accelerates tumor progression due to carcinogenesis. In glioma, partial loss of MYCBP was found to significantly improve the overall survival rate of the patients (37). In ESCC, miR-26a depressed tumor cell proliferation by inhibiting MYCBP expression (22). In addition, in hepatocellular carcinoma, EYA4 alleviated tumor progression by inhibiting MYCBP (36). In the present study, our results indicated that MYCBP was upregulated in CRC tissues and cells. The carcinogenic effects of MYCBP were further verified. Bioinformatics and luciferase reporter analyses showed that MYCBP was negatively targeted by miR-495-3p, and further functional verification indicated that LUNAR1 accelerated CRC cell proliferation,

migration and invasion, and inhibited cell apoptosis via the miR-495-3p/MYCBP axis.

In summary, our findings demonstrated that LUNAR1 was highly expressed in CRC tissues and cell lines and was negatively associated with overall survival of CRC patients. LUNAR1 knockdown accelerated cell apoptosis and inhibited CRC cell proliferation, migration and invasion. Moreover, LUNAR1 functioned as a sponge of miR-495-3p; miR-495-3p overexpression inhibited CRC cell proliferation, migration and invasion, and depressed cell apoptosis by negatively targeting MYCBP. Collectively, LUNAR1 accelerates CRC progression through the miR-495-3p/MYCBP axis. Our findings indicate that LUNAR1 acts as a prognostic biomarker for CRC patients.

Acknowledgements

Not applicable.

Funding

Not applicable.

Availability of data and materials

The raw data supporting the conclusions of this manuscript will be made available by the authors, without undue reservation, to any qualified researcher.

Authors' contributions

JQ and QS conceived and designed the study. AG, FL and KX performed the experiments. JQ and QS wrote the paper. AG, FL and KX reviewed and edited the manuscript. All authors read and approved the manuscript and agree to be accountable for all aspects of the research in ensuring that the accuracy or integrity of any part of the work are appropriately investigated and resolved.

Ethics approval and consent to participate

All patients were informed before their inclusion; written consent of the patients was obtained. All experimental protocols were approved by the Ethics Committee of The First Affiliated Hospital, College of Medicine, Zhejiang University (Zhejiang, China; ethical approval no. PRO20180916-R1) and experimental procedures were conducted according to the Declaration of Helsinki Principles.

Patient consent for publication

Not applicable.

Competing interests

The authors declare that they have no competing of interests.

References

1. Wang Y, Lina L, Xu L, Yang Z, Qian Z, Zhou J and Suoni L: Arctigenin enhances the sensitivity of cisplatin resistant colorectal cancer cell by activating autophagy. Biochem Biophys Res Commun 520: 20-26, 2019.
2. Lech G, Słotwiński R, Słodkowski M and Krasnodębski IW: Colorectal cancer tumour markers and biomarkers: Recent therapeutic advances. World J Gastroenterol 22: 1745-1755, 2016.
3. Tauriello DV, Calon A, Lonardo E and Batlle E: Determinants of metastatic competency in colorectal cancer. Mol Oncol 11: 97-119, 2017.
4. Zeng A, Hua H, Liu L and Zhao J: Betulinic acid induces apoptosis and inhibits metastasis of human colorectal cancer cells in vitro and in vivo. Bioorg Med Chem 27: 2546-2552, 2019.
5. Liu Y, Xu L, Lu B, Zhao M, Li L, Sun W, Qiu Z and Zhang B: LncRNA H19/microRNA-675/PPARα axis regulates liver cell injury and energy metabolism remodelling induced by hepatitis B X protein via Akt/mTOR signalling. Mol Immunol 116: 18-28, 2019.
6. Li D, Wang J, Zhang M, Hu X, She J, Qiu X, Zhang X, Xu L, Liu Y and Qin S: LncRNA MAGI2-AS3 is regulated by brd4 and promotes gastric cancer progression via maintaining ZEB1 overexpression by sponging miR-141/200a. Mol Ther Nucleic Acids 19: 109-123, 2020.
7. Wang R, Li Y, Du P, Zhang X, Li X and Cheng G: Hypomethylation of the lncRNA SOX21-AS1 has clinical prognostic value in cervical cancer. Life Sci 233: 116708, 2019.
8. Han Y, Hu H and Zhou J: Knockdown of LncRNA SNHG7 inhibited epithelial-mesenchymal transition in prostate cancer though miR-324-3p/WNT2B axis in vitro. Pathol Res Pract 215: 152537, 2019.
9. Cheng Y, Wu J, Qin B, Zou BC, Wang YH and Li Y: CREB1-induced lncRNA LEF1-AS1 contributes to colorectal cancer progression via the miR-489/DIAPH1 axis. Biochem Biophys Res Commun 526: 678-684, 2020.
10. Chuo D, Liu F, Chen Y and Yin M: LncRNA MIR503HG is downregulated in Han Chinese with colorectal cancer and inhibits cell migration and invasion mediated by TGF-β2. Gene 713: 143960, 2019.
11. Wang Y, Jiang F, Xiong Y, Cheng X, Qiu Z and Song R: LncRNA TTN-AS1 sponges miR-376a-3p to promote colorectal cancer progression via upregulating KLF15. Life Sci 244: 116936, 2020.
12. Trimarchi T, Bilal E, Ntziachristos P, Fabbri G, Dalla-Favera R, Tsirigos A and Aifantis I: Genome-wide mapping and characterization of Notch-regulated long noncoding RNAs in acute leukemia. Cell 158: 593-606, 2014.
13. Peng W and Feng J: Long noncoding RNA LUNAR1 associates with cell proliferation and predicts a poor prognosis in diffuse large B-cell lymphoma. Biomed Pharmacother 77: 65-71, 2016.
14. Zhang Z, Li G, Qiu H, Yang J, Bu X, Zhu S, Zheng J, Dang C, Wang W and Chu D: The novel notch-induced long noncoding RNA LUNAR1 determines the proliferation and prognosis of colorectal cancer. Sci Rep 9: 19915, 2019.
15. Hawkins LJ and Storey KB: MicroRNA expression in the heart of Xenopus laevis facilitates metabolic adaptation to dehydration. Genomics 112: 3525-3536, 2020.
16. Tu Y, Ma T, Wen T, Yang T, Xue L, Cai M, Wang F, Guan M and Xue H: MicroRNA-377-3p alleviates IL-1β-caused chondrocyte apoptosis and cartilage degradation in osteoarthritis in part by downregulating ITGA6. Biochem Biophys Res Commun 523: 46-53, 2020.
17. Li D, Knox B, Chen S, Wu L, Tolleson WH, Liu Z, Yu D, Guo L, Tong W and Ning B: MicroRNAs hsa-miR-495-3p and hsa-miR-486-5p suppress basal and rifampicin-induced expression of human sulfotransferase 2A1 (SULT2A1) by facilitating mRNA degradation. Biochem Pharmacol 169: 113617, 2019.
18. Zhou T, Wu L, Ma N, Tang F, Zong Z and Chen S: LncRNA PART1 regulates colorectal cancer via targeting miR-150-5p/miR-520h/CTNNB1 and activating Wnt/β-catenin pathway. Int J Biochem Cell Biol 118: 105637, 2020.
19. Xia D, Yao R, Zhou P, Wang C, Xia Y and Xu S: LncRNA NEAT1 reversed the hindering effects of miR-495-3p/STAT3 axis and miR-211/PI3K/AKT axis on sepsis-relevant inflammation. Mol Immunol 117: 168-179, 2020.
20. Lin L, Tong G, Li M, Liu A and Wang S: MiR-495-3p facilitates colon cancer cell proliferation via Wnt/β-catenin signaling pathway by restraining Wnt inhibitory factor. Trop J Pharm Res 16: 2113, 2017.
21. Jung HC and Kim K: Identification of MYCBP as a beta-catenin/LEF-1 target using DNA microarray analysis. Life Sci 77: 1249-1262, 2005.
22. Li J, Liang Y, Lv H, Meng H, Xiong G, Guan X, Chen X, Bai Y and Wang K: miR-26a and miR-26b inhibit esophageal squamous cancer cell proliferation through suppression of c-MYC pathway. Gene 625: 1-9, 2017.

23. Gong L, Xia Y, Qian Z, Shi J, Luo J, Song G, Xu J and Ye Z: Overexpression of MYC binding protein promotes invasion and migration in gastric cancer. Oncol Lett 15: 5243-5249, 2018.
24. Dong SM, Cui JH, Zhang W, Zhang XW, Kou TC, Cai QC, Xu S, You S, Yu DS, Ding L, *et al*: Inhibition of translation initiation factor eIF4A is required for apoptosis mediated by Microplitis bicoloratus bracovirus. Arch Insect Biochem Physiol 3: 96, 2017.
25. Cui JH, Dong SM, Chen CX, Xiao W, Cai QC, Zhang LD, He HJ, Zhang W, Zhang XW, Liu T, *et al*: Microplitis bicoloratus bracovirus modulates innate immune suppression through the eIF4E-eIF4A axis in the insect Spodoptera litura. Dev Comp Immunol 95: 101-107, 2019.
26. Pulito C, Mori F, Sacconi A, Goeman F, Ferraiuolo M, Pasanisi P, Campagnoli C, Berrino F, Fanciulli M, Ford RJ, *et al*: Metformin-induced ablation of microRNA 21-5p releases Sestrin-1 and CAB39L antitumoral activities. Cell Discov 3: 17022, 2017.
27. Chen L, Zhu M, Yu S, Hai L, Zhang L, Zhang C, Zhao P, Zhou H, Wang S and Yang X: Arg kinase mediates CXCL12/CXCR4-induced invadopodia formation and invasion of glioma cells. Exp Cell Res 389: 111893, 2020.
28. Pei G, Xu L, Huang W and Yin J: The protective role of microRNA-133b in restricting hippocampal neurons apoptosis and inflammatory injury in rats with depression by suppressing CTGF. Int Immunopharmacol 78: 106076, 2020.
29. Li Z, Cao Y, Jie Z, Liu Y, Li Y, Li J, Zhu G, Liu Z, Tu Y, Peng G, Lee DW and Park SS: miR-495 and miR-551a inhibit the migration and invasion of human gastric cancer cells by directly interacting with PRL-3. Cancer Lett 323: 41-47, 2012.
30. Ahmed EM, Hassan MSA, El-Malah AA and Kassab AE: New pyridazine derivatives as selective COX-2 inhibitors and potential anti-inflammatory agents; design, synthesis and biological evaluation. Bioorg Chem 95: 103497, 2020.
31. Zhou Z, Zhu Y, Gao G and Zhang Y: Long noncoding RNA SNHG16 targets miR-146a-5p/CCL5 to regulate LPS-induced WI-38 cell apoptosis and inflammation in acute pneumonia. Life Sci 228: 189-197, 2019.
32. Zhao G, Zhang L, Qian D, Sun Y and Liu W: miR-495-3p inhibits the cell proliferation, invasion and migration of osteosarcoma by targeting C1q/TNF-related protein 3. Onco Targets Ther 12: 6133-6143, 2019.
33. Zhao Y, He J, Gao P, Niu Y, Zhang J, Wang L, Liu M, Wei X, Liu C, Zhang C, *et al*: miR-769-5p suppressed cell proliferation, migration and invasion by targeting TGFBR1 in non-small cell lung carcinoma. Oncotarget 8: 113558-113570, 2017.
34. Kuipers EJ, Grady WM, Lieberman D, Seufferlein T, Sung JJ, Boelens PG, van de Velde CJ and Watanabe T: Colorectal cancer. Nat Rev Dis Primers 5: 15065, 2015.
35. Liu L, Wang HJ, Meng T, Lei C, Yang XH, Wang QS, Jin B and Zhu JF: lncRNA GAS5 inhibits cell migration and invasion and promotes autophagy by targeting miR-222-3p via the GAS5/PTEN-signaling pathway in CRC. Mol Ther Nucleic Acids 17: 644-656, 2019.
36. Ma D: 153P-Exosomal LINC00174 facilitates epithelial-mesenchymal transition in residual hepatocellular carcinoma after insufficient radiofrequency ablation by regulating c-JUN/MYCBP/c-Myc axis. Ann Oncol 30 (Suppl 9): ix53-ix54, 2019.
37. Lehrer S, Rheinstein PH and Rosenzweig KE: Loss of MycBP may be associated with the improved survival in 1P co-deletion of lower grade glioma patients. Clin Neurol Neurosurg 172: 112-115, 2018.

This work is licensed under a Creative Commons Attribution-NonCommercial-NoDerivatives 4.0 International (CC BY-NC-ND 4.0) License.